Ultimate Strength of Parabolic Concrete Arches

Adnan S. Alkuaity[1]

[1]Department of building and construction technology, Islamic University

***Abstract*— This investigation is aimed to present a simple analytical approach for predicting the ultimate strength of concrete arch using theory of plasticity. Six models of two-hinged parabolic concrete arches with and without steel reinforcement were tested under concentrated load. The observed behavior of cracking strength and collapse load of the arches tested were compared with those predicted by the analytical procedure proposed here. The arches tested were un-reinforced concrete, lightly reinforced concrete, and concrete with filing iron respectively. A Good agreement is found between the proposed analysis and test results. Tests have shown that the collapse of all arches was mainly due to the formation of two plastic hinges at a point of maximum bending moment which is similar to collapse mechanism adopted in this study. The use of light concentric steel reinforcement resulted into a significant increase in the ultimate load. This increase reaches up to three times of that without reinforcement. Ductility was also found to be greatly improved due to using steel reinforcement in arches. The procedure of analysis in this paper can give a simple guide for design of concrete arch.**

***Index Terms*— Plastic analysis, parabolic arch, reinforced concrete, design**

I. INTRODUCTION

The arches possess a unique property to resist loads primarily by direct compression stress rather than by flexural or shear stress. For long spans such a property could result to more economical structure than other types of structures. This encourages the old builder and the structural engineers at the past till now to build beautiful structures round the word. Previously, the arch proved to be one of the few structural systems which make it efficient to cover large spans with various types of brick stones such as stone bridges etc.

The top surface of the arch can be made flat surface either by fill materials or by building secondary skeleton on the arch to meet the functional requirements of the arch. However, the parabolic arch has further advantage compared to circular arch, because, the parabolic arch can transfer the uniformly distributed loads directly by compression through its own center line. Unlike other types of arches, the parabolic arch gives lesser rise than circular for specific span. On the other hand, parabolic arch will require less fill materials and hence results extra saving in materials. Therefore, parabolic arch is adopted in this study.

The arch is usually designed in such a way that the predominant loading will produce a uniform compression stress through sections of arch whereas the bending moment results from other loading conditions should be kept minimal. Generally, an arch has to support its own self-weight and additional live loads safely. Usually, the point loads have a thrusting nature and can cause collapses when their action moves the thrust line out of the arch, generating plastic hinges. On the other hand, the self-weight in catenary arch could offer a resistance to any mechanism of collapse. However, the principle of the design of any arch is aimed to keep the thrust line with in the arch thickness. This will be solved by using a parabolic shape of arch which is very near to catenary

Extensive experimental and analytical research work have been done on circular masonry arches which interested in collapse load and mode of failure. Heyman explained for the first time the applicability of ultimate load theory for any masonry loadbearing structure. (1966) [1], (1969) [2], assuming no *sliding failure, no tensile strength* in masonary and *the masonry has infinite compression strength*. The collapse mechanism of the arch is identified by the progressive formation of hinges that coincide with the points where the thrust line is tangent to the intrados or extrados of the arch. This method was applied by Hendry (1985)[3].

A particular closed-form approach has been recently developed by Milani (2007) [4] and Audeneart (2009)[5],(2010)[6]. This method is based on the fundamental theorems of limit analysis and is used to determine the critical ints with a relatively small modeling effort. To assure the stability of the masonry arch bridges, a model based on equilibrium equations and compatibility conditions is first developed. Next, the material properties are added to determine the formation of the hinges.

The mechanism for formation of hinges is not the only possible for the arch, but the experimental studies of Hendry [7] show that it can be considered as the most likely collapse mechanism for arches well buttressed.

Tao, H., (2003) [8] predicted ultimate load by finite element simulation of open spandrel brickwork masonry arch bridges which was directly proportional to the tensile strength.

Garrity (2010) [9] applied near-surface reinforcement as a minimum intervention, minimum disruption repair or strengthening technique for masonry arch bridges and similar structures. The reinforcement was used to resist tensile stresses developing in arch besides improving ductility.

Recently, researches focused on the finite element methods for predicting the behavior of arch (2018),[10]. However, such methods may not always available at the hands of the designers. The aim of this study is to introduce a simple analytical procedure which can correlate the failure load of parabolic arch with section properties of arch using theory of plasticity.

This investigation aimed to present simple analytical approach for predicting the ultimate strength of concrete arch using theory of plasticity. The procedure could be considered as a guide for design of parabolic arch. Test results of six models of unreinforced concrete arches, reinforced concrete arches and concrete with iron fillings are tested and compared with the proposed analysis.

II. THEORETICAL CONSIDERATIONS

In this analysis, a two-hinged parabolic tied arch shown in Figure1 is considered. Parabolic shape is similar to the catenary in which the uniformly distributed load transfers to the supports by axial thrust through its own center line. Therefore, the parabolic shape of the arch will produce only axial compression in the arch under uniformly distributed load. Referring to figure1 , the equation of axis of the arch can be expressed by the following equations:

$$y = \frac{4h}{L}\left(x - \frac{x^2}{L}\right) \qquad (1)$$

$$\frac{dy}{dx} = \frac{4h}{L}\left(1 - \frac{2x}{L}\right) \qquad (2)$$

Where:
L is the span of the arch
h is maximum rise of the arch
P = concentrated load

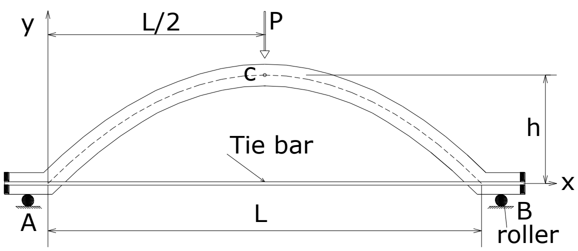

Fig. 1 Two-hinges parabolic arch

On the other hand, when this arch is subjected to either partially distributed load or concentrated load (P) as the general case in practice, bending moments besides the axial compressive force will be developed in the arch sections. The elastic analysis of such a case can be made in two stages, namely, elastic stage at non-cracked section and plastic analysis at ultimate stage. These cases can be summarized here.

A. *Elastic analysis*

Referring to Figure1, as the applied load develops tensile stress of magnitude less than the tensile strength of concrete then the section will act as non-cracked section and elastic theory can be used to determine reactions and deformations. In this case, the redundant horizontal force (H) developed in the tie rod can be found using virtual work method. Neglecting the small effect of shear and axial strain, the horizontal force H in the tie bar can be derived

It is known from Castiglione's First Theorem that the partial derivative of the total strain energy in any structure with respect to the applied force or moments gives the displacement or rotation respectively at the point of application of the force or the moment in the direction of the applied force or moment. However, when the supports do not yield, the partial derivative of the total strain energy with respect to the horizontal thrust will be zero. If the supports yield by an amount δ in the direction of the horizontal thrust, then the partial derivative of total strain energy with respect to the horizontal thrust will be equal to δ. Neglecting strain energy due to direct thrust which is small, total strain energy due to bending moment will be:

$$U = \int \frac{M^2}{2EI} ds + \int \frac{N^2}{2AE} ds \qquad (1)$$

Where
M = the bending moment
N = axial load
A = cross sectional area of arch
E = modulus of elasticity

$$\frac{\partial u}{\partial H} = -\delta \qquad (2)$$

For tied arch with constant EI, $I = I_c \sec\theta$, $ds = dx \sec\theta$, where I_C is the moment of inertia at the crown section. Then, the horizontal force in the tie can be derived from equation 1 and 2 as:

$$H = \frac{\int M y ds - EI\delta}{\int y^2 ds} = \frac{\int M y dx - EI\delta}{\int y^2 dx} \qquad (3)$$

Where M is the bending moment due to concentrated load (P) assuming H=0.
For the arches tested here, h=250mm, L=1000mm, the force in the tie bar H can be determined as:

$$H = 0.776P \qquad (4)$$

Using STAAD/PRO computer program (11), the bending moment diagram, shear force diagram and direct force diagram are shown in Figure 2.

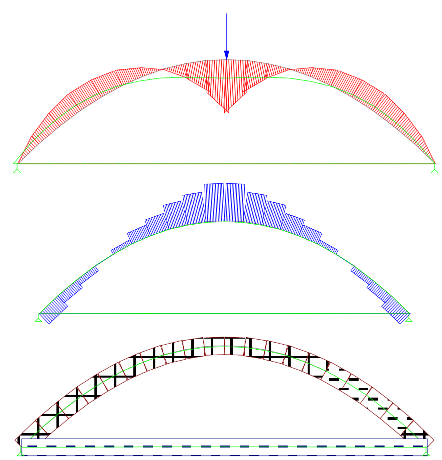

a-Bending moment b- Shear force
c- Axial force diagram

Fig. 2 bending moment diagram, shear force diagram and direct force diagram

B. *Cracking load*

When the tensile stress develops due to applied load exceeds the tensile strength of the arch, cracks will takes place. Then concrete does not respond elastically to loads after formation of the first crack. That results a certain inconsistency in designing reinforced cross-sections by ultimate strength methods when the moments for which those sections are being designed have been determined by elastic analysis.
The tensile stress produced by applied load can be determined as:

$$f = \frac{N}{A} \pm \frac{MC}{I} > \text{ft} \quad (5)$$

Where:
f = tensile stress due to applied load (it can be taken between 10-15% of compressive strength)
N = axial load
M = bending moment at the section
C = distance from extreme fiber to the neutral axis
I = second moment of inertia of the section
ft = tensile strength of concrete

C. Plastic analysis

As the applied load at the mid-span increases the first plastic hinge develops in the arch at point of maximum bending moment under the point load. This hinge will redistribute the bending moment in the arch as shown in Figures 2 a, b. The further increase in the applied load will develop a second plastic hinge at the location of new maximum bending moments resulting collapse of the arch. The position of second plastic hinge is found to be at the midway between the point load and the right support.
The worst position of live load was investigated to be at about quarter span as shown in Figure 3c. In this case the first plastic hinge will form under point load (Figure 3d) and the second plastic hinge assumed to be formed at maximum bending moment after redistribution which is about the midway between the point load and the right support as shown in Figure 3d. These locations would be compared with those derived mathematically by Heyman (1971).

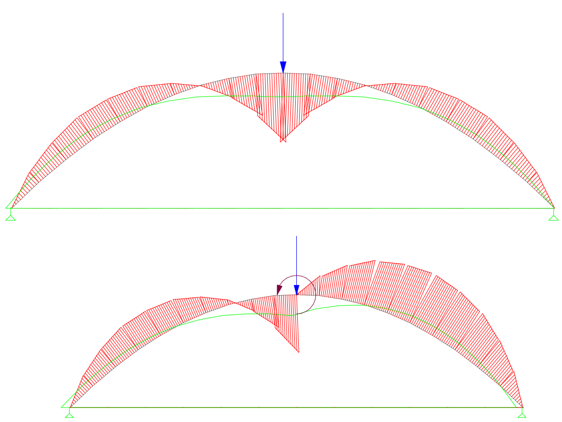

(a) (b)
Fig. 3 Bending moment diagram load at mid-span a-elastic stage b-at plastic stage

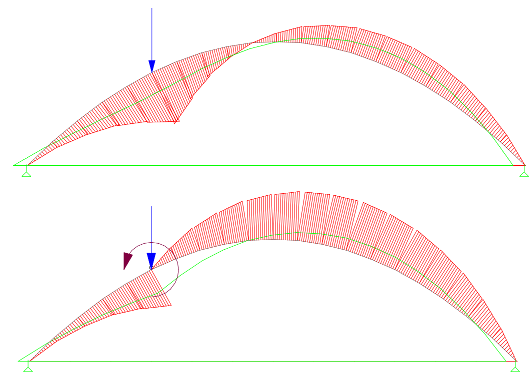

(c) (d)
Fig. 4 Bending moment diagram load at quarter-span (c)-elastic stage (d)-at plastic stage

Generally, the arch section can be subjected to combination of compressive and tensile stresses under loads. In plastic analysis, the plastic hinge is assumed to transfer plastic moment in amount depending on the sectional properties of the arch. As suggested by Heyman, (1966) [1] and Heyman, (1969) [2] for the masonry structure, the plasticity theory can predict the non-elastic behavior unreinforced concrete arches using collapse mechanism shown in Figure.(4). Using the work equation for the collapse mechanism shown in figure 4. the plastic moment Mp was derived by Heyman (1971) [11] as;

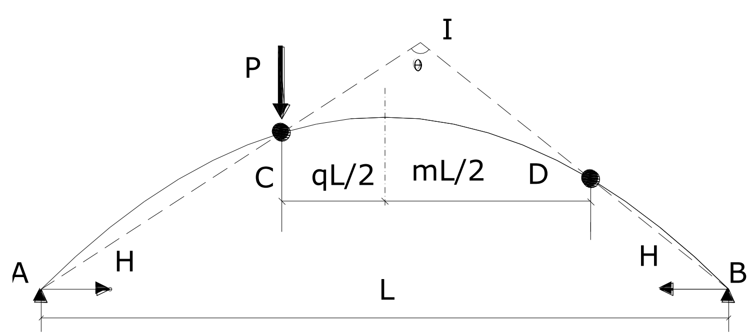

Fig. 5 Collapse mechanism of two –hinge arch

From work equation as:

$$\text{Mp} = \frac{PL}{4}(1\text{-q})\,\frac{[q+m(1-q)-m^2]}{[(2-q\,)+m(1-q)-m^2]} \quad (6)$$

For the case of concentrated load at mid-span equation 6 show, the right plastic hinge lies exactly half-way between point load and right-hand support.
With assumption of a constant plastic hinge moment Mp of the collapse mechanism shown in Figure (4), the unsafe theorem state that the value of Mp in equation 6 must be maximized with respect to m, this condition gives

$$\text{m} = \frac{1}{2}(\,1-q) \quad (7)$$

This means that the hinge point lies exactly halfway (horizontally) between the point load and the right-hand support. Then, Mp becomes,

$$\text{Mp} = \frac{PL}{4}(1\text{-q})\,\frac{(1+q\,)^2}{(3-q\,)^3} \quad (8)$$

DOI: http://doi.org/10.24086/aces2020/paper.183

The critical position of point load can be found by maximizing Mp with respect to q

$q = \frac{5-\sqrt{20}}{2} = 0.264$ (9)

That is means when the point load at about quarter the span

Mp max.= (0.0451)PL (10)

In the arches tested here, the concentrated load is applied at the mid-span (q=0). With L=1m Mp becomes:

Mp = PL/36 = 0.0272PL (11)

Use equilibrium equation to find horizontal reaction H as:

H = (8/9) P (12)

To find the position of point load to give maximum moment in the arch, Mp in equation 6 should be maximized with respect to q. The value of q = 0.528 and maximum Mp is:

Mp max.= 0.0451PL (13)

D. Plastic moment and collapse load

The most important parameter required for prediction of collapse load of the arch is the plastic hinge of the section. Knowing the plastic moment of the arch section, the design of arch would be simple problem. In this investigation, the plastic moment for unreinforced and reinforced concrete section is evaluated.

- Singly reinforced concrete section

The stress block at ultimate stage of loading is assumed as shown in Figure 5. The axial force N and the plastic moment Mp at the section can be evaluated as:

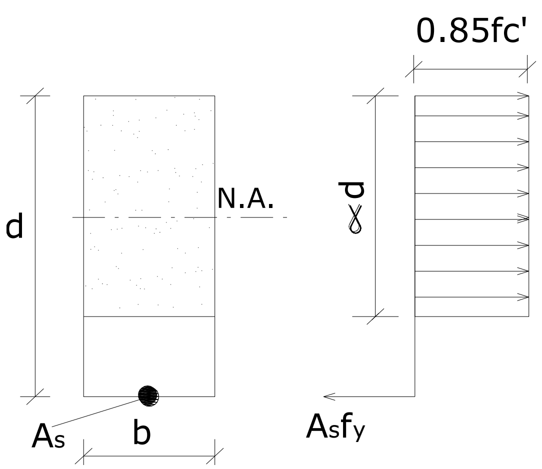

Fig. 6 Stress distribution at plastic stage

$N = f_yA_s - \alpha\,(0.85f'_c)\,b\,d$ (14)

$M_p = f_yA_s(d/2) + 0.85f'_c)\,\alpha\,(\frac{bd^2}{2})\,(1-\alpha)$ (15)

Negative sign indicates the compressive stress while positive sign is tensile stress

Where

A_s = area of steel

f'_c = crushing strength of the concrete

f_y = yield strength of the steel.

h = depth of the section.

Mp = bending moment.

N = axial compression force.

α = ratio between depth of compression stress block to the total depth.

For the case of the test arches where the point load is at mid span, Mp = 0.0272 P L and N will equal to H = (8/9) P. Substitute these in equations 13 and 14 and simplify these equations to get:

$\mathbf{N = (0.85f'_c)\,b\,d\,(\rho\,\frac{f_y}{0.85f_{c'}} - \alpha)}$ (15)

$\mathbf{M_p = (\frac{1}{2}\,bd^2)\,(0.85f'_c)\,[\rho\,\frac{f_y}{0.85f_{c'}} + \alpha\,(1-\alpha)]}$ (16)

After determining Mp, the collapse load (P) of the arch is found from equation 11:

Where

$\rho = A_s / (bd)$

b = width of section

d = height of section

- Un-reinforced concrete

For the un-reinforced section, let ρ = 0 in equations 15 and 16 to get:

$N = -\alpha\,(0.85f'_c\,b\,d)$ (17)

$M_p = -(\frac{1}{2})\,bd^2\,(0.85f'_c)\,[\alpha\,(1-\alpha)]$ (18)

(α) isevaluated from test results by substituting equation 12 in equation 17 to be approximately constant of about 0.054.

Let α = 0.054 in equations 17, 18:

$N = -0.054\,(f'_c\,b\,d)$ (19)

$M_p = -0.946\,N\,(\frac{1}{2}\,d)$ (20)

To get collapse load P, Substitute equation 19 and equation 12 in equation 20:

$\mathbf{P = [0.61\,f_{cu}\,bd^2] / L}$ (21)

Where fc' = 0.67 fcu

Same procedure could be followed to get collapse load of parabolic arch with concentrated load at the quarter point of the span.

- Doubly reinforced concrete section

For the doubly reinforced section or centrally reinforced section subjected to bending moment and axial loads, the plastic moment can be derived using same principle.

For centrally reinforced section, collapse load can be derived as:

$N = -\alpha\,(f'_c\,b\,d)$ (22)

At ultimate stage

N = H = (8/9) P

$\mathbf{M_p = N\,(\frac{1}{2}\,d)\,(1-\alpha)}$ (23)

After determining Mp, the collapse load (P) of the arch is found from equation 11

III. Experimental Investigation

To study the behavior of a concrete parabolic arch under concentrated load, three groups of arches were tested. The cross-sectional area of all arches was 100mm wide, and 50mm depth. The shapes of arches are parabolic with span 1000mm and maximum rise of 250mm. Only one concrete mix with proportion of (cement: sand: crushed stone) 1:1:2.4 was used throughout using a water cement ratio of 0.5. The coarse aggregate used was crushed stone with 12mm nominal size. The sample of test specimen is given in Figure 6.

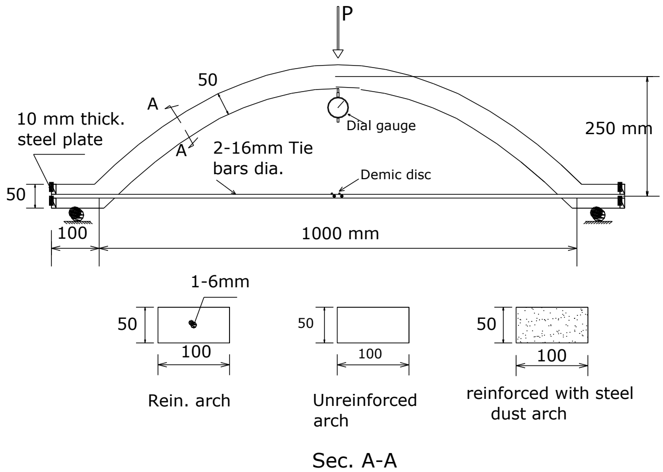

Fig. 7 Test specimens

TABLE I
TEST PROGRAM

Group	Arch no.	Reinforcement Type	Steel percentage	Tie bars
A	AP1 AP2	Plan concrete	0	2-6mm dia
B	AR1 AR2	1-6mm dia.	0.56	2-6mm dia
C	AS1 AS2	Steel dust	0.5% by volume	2-6mm dia

Summary of test specimens details are given in Table 1. Group A consist of two identical arches cast with plain concrete. Group B includes another two identical arches reinforced with 1Φ6 at centroid of section as shown in Fig.8. The arches in group C are cast with 0.5% iron filling by volume. The yield strength of the steel bar in group B is 275N/mm^2.
In all arches the horizontal movement of the supports was prevented using 2Φ6 mm tie bars. These bars also used to measure axial strain by which the horizontal reaction at the support was determined through loading test. Deflection under point load was measured for each arch tested using mechanical dial gouge. The samples of test specimens are shown in Figure 12

A. *Concrete strength*

Compressive strength was determined by testing six cubes 150x150x150 mm each according to ASTM specifications. Three cubes were tested at age 7 days and another three at age 28 day. Tensile splitting strength was found by testing six cylinders 300mm height x150mmdiameter each.

Flexural tensile strength was also determined by testing prisms 100x100x500 mm dimensions. Summary of test results is given in Table 2.

TABLE 2
CONCRETE STRENGTH

Mix type	Arch	Compressive strength (N/mm²) 7-day 28-day	Tensile strength (N/mm²) 7-day 28-day	Flexural strength (N/mm²) 7-day 28-day
Plain concrete arch	AP1 AP2	26.9 35.0 31.5 39.0	2.8 3.1 3.0 3.3	5.7 6.3 5.9 6.5
Reinforced concrete	AR1 AR2	24.9 36.0 21.3 32.0	2.7 3.2 2.5 3.0	6.0 6.9 5.0 6.7
Concrete with iron filings	AS1 AS2	27.0 31.1 30.0 36.0	2.1 2.8 2.3 3.0	3.9 5.0 4.1 5.2

IV. RESULTS AND DISCUSSION

A. *Load deflection curves*

The mid-span deflections were measured for all arches at each increment of loading. Load –deflection curves were plotted in Figure 7 for specimens AP1, AR1, AP1. These samples represents plain concrete arch AP1 and reinforced concrete arch AR1 and iron filling concrete arch AP1. It can be observed that the deflection is of all arches is linearly proportional to the applied load at initial stage of loading.
Figure 7 shows that the stiffness of un-reinforced arches is slightly higher than that of reinforced arch. This may be due to the variation in concrete strength of the specimens. Reinforced concrete arch showed very ductile behavior than un-reinforced arches. The ultimate deflection of reinforced arch is about eight times that of unreinforced arches. That belongs to the presence of 0.56% steel reinforcement which is greatly improved the ductility of the arch compared to un-reinforced arches.
The stiffness of reinforced arch was further reduced after initiation of the first crack as in flexural beam.

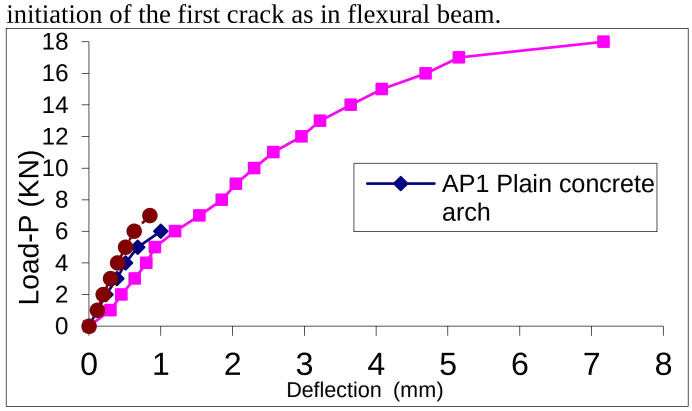

Fig. 8 Load-Deflection curves

DOI: http://doi.org/10.24086/aces2020/paper.183

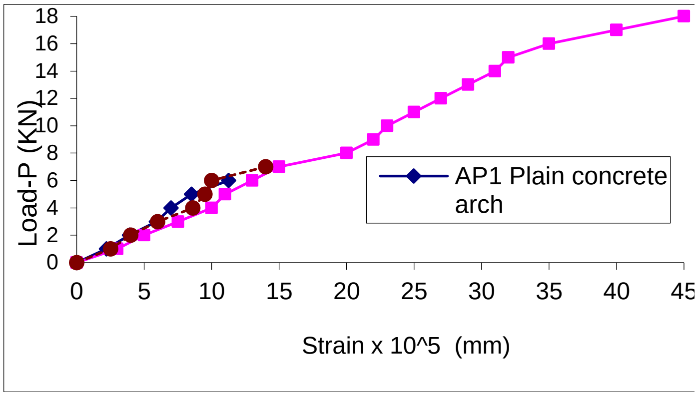

Fig. 9 Load-Tie strain curves

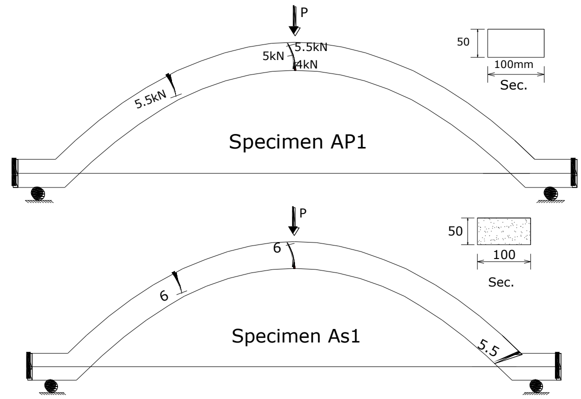

Fig. 10 cracking behavior of un-reinforced concrete AP1and AP2

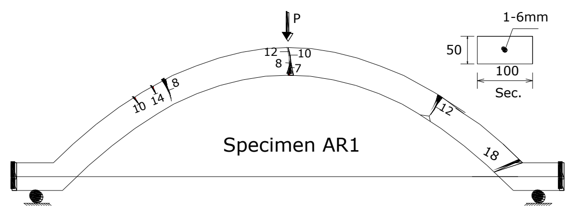

Fig. 11 Cracking behavior of reinforced concrete arch AR1

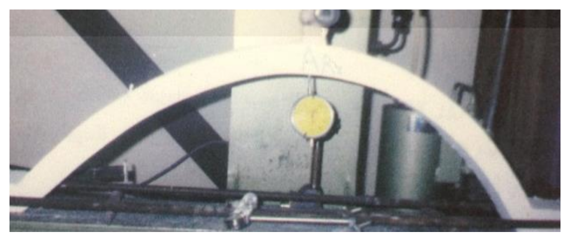

Fig. 12 Preparing arch (AR1) under test

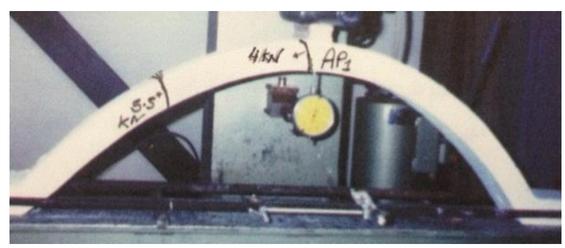

Fig. 13 Cracking at arch (AP1) during test

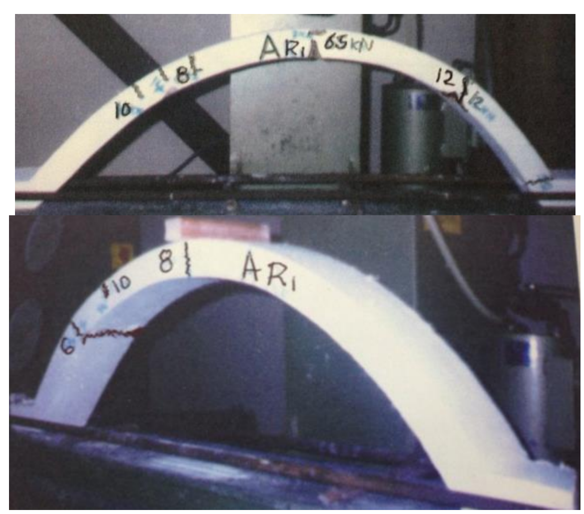

B. Cracking behavior and mode of failure

In all arches, when the point load was gradually increased from zero to that magnitude at which the arches failed, two main flexural cracks were clearly distinguished. The first crack occurred under the point load (point of maximum positive bending moment see Figure 2a) which initiated in the bottom fiber and propagated upward close to the top fiber. Further increase in the applied load developed a second flexural crack in the top fiber lies approximately half-way (horizontally) between the loading point and the left support (point of maximum negative bending moment). For unreinforced arches (AP)., further increase in the applied load caused a sudden brittle failure in arches whereas very ductile failure has seen in reinforced arches. However the positions of cracks indicates the formation of plastic hinge which formed in sequence similar to that suggested in Figures 2,3. The first cracking load is approximately represented 90% of ultimate load whereas in reinforced arch the first cracking load is about 50% of ultimate load. From design point of view, the first cracking load could be considered as ultimate load.

After formation the second crack (AR), the reinforced arches were capable to sustain higher load accompanied by more fine cracks which distributed on the left and right of the second major cracks. At ultimate stage of loading, the second crack stated from top fiber then it penetrated deeply downward as the load increased resulting in to crushing of bottom fiber (compression zone). This show that the development of plastic hinge at this section is converted the arch into a mechanism. For unreinforced arches, the failure was very brittle whereas a more ductile behavior was observed in the reinforced arches.

Figure 13 Failure mode of arch (AR1)

C. Comparison

Generally, tests showed that the collapse mechanism of unreinforced and reinforced arches were similar to that proposed by plastic analysis mentioned earlier and conform the suggested models in this study Figures 2,3.
A comparison was made between the test results of the first cracking load, second cracking load and failure load of the arches and those predicted by the theoretical analysis proposed in this investigation, as given in Table 3.
The theoretical first cracking load is calculated based on equation 5, whereas, the ultimate loads were calculated using proposed equations 21,23.As given in Table 3, the ratio between tested to calculated first flexural cracking load was between 0.73 and 1.36, whereas that for ultimate load varied between 0.86 to 1.09.
The results of this investigation have shown that ratio between ultimate loads proposed in this study and those observed in the tests was ranging between about 0.73 and 1.28. This means the proposed approach can predict the ultimate capacity of reinforced and un-reinforced arches with reasonable accuracy.
Figure 8, shows the relationship between the applied load and the horizontal tie force H in the supports. It can be observed that the tie force H is directly proportional with applied load which confirms with equations 4, 12 proposed here.
However, the proposed procedure can be adopted as an adequate guide for predicting the behavior of both un-reinforced and reinforced concrete arches under point loading. Further tests are required to cover other parameters which affect the strength of reinforced concrete arches.

TABLE 3
CRACKING LOADS AND ULTIMATE LOADS OF TEST ARCHES

Arch	First cracking load kN 1	Theoret-ical cracking load 2	Theo. Crack. load/test crack. Load 3	Test Ultimate load kN 4	(Cracking load) / (Ultimate load) 5	Proposed method Ultimate load kN 6	Test/Theoretical Ratio 7
AP 1	4.0	3.6	0.9	5.5	0.65	5.34	1.03
AP 2	4.0	3.9	0.98	6.0	0.67	5.95	1.01
A R1	6.5	3.7	0.55	18.0	0.36	21.4	0.84
A R2	8.0	3.2	0.4	15.0	0.53	20.6	0.73
AS 1	5.5	3.2	0.58	6.0	0.92	4.74	1.27
AS 2	7.0	3.7	0.53	7.0	1.0	5.49	1.28

6. CONCLUSIONS

Six concrete models of two-hinged parabolic tied arches with and without reinforced were tested under point loading. A comparison was made between ultimate load and that predicted by the analysis proposed in this study. Although few specimens were tested in this investigation, some conclusions may be drawn as:
1- The first cracking load of unreinforced arch is about 90% of its own ultimate load ,whereas, in reinforced arch the cracking load is about 50% of its own ultimate load. Therefore the first cracking load in unreinforced arch may be considered as the useful load capacity of arch.
2-The positions of plastic hinges in all arches tested here are nearly same as those suggested by the proposed analysis in this study.
3-The mode of failure of unreinforced arches was due to penetration of two major tensile crack into whole depth of the arches whereas a compression failure of the compression zone was observed in reinforced concrete arches.
4-The use of 0.56% concentric steel resulted into great increase in the ultimate load. The increase reaches up to about three times as much as those of unreinforced arches. Ductility was also greatly improved due to concentric reinforcement.
5-The theoretical analysis proposed in this paper was found to be applicable to predict the collapse loads of both un-reinforced and reinforced concrete arches tested here with good accuracy.
6-Adding of iron filling to concrete has no significant effect on the behavior of the unreinforced arches.

REFERENCES

1- J. Heyman, "The stone skeleton" Structural Engineering of Masonry Architecture", University of Cambridge Press, Cambridge, 1966.
2-Heyman, J. "The safety of masonry arches" Int. J. mech. Sci., 11, 1969.

3- A.H. Hendry, S.R. Davies, R. Royles, Test on a Stone, Masonry Arch at Bridgemill-Girvan, Transport and Road Research Lab, Contractor Report 7, UK,1985.
4- G. Milani, A simple equilibrated homogenization model for the limit analysis of masonry structures. Wseas Transactions on Applied and Theoretical Mechanics, Issue 5, Vol. 2, 2007, pp. 119-125.
5- A. Audeneart, W. Dullaert, G. Reniers , H. Peremans, Evaluation of the limit load capacity of masonry arch bridges, Wseas Transactions on Applied and Theoretical Mechanics, Issue 4, Vol. 4, 2009, pp. 137-146.
6- A. Audeneart A., J. Beke, Applicability analysis of 2D-models for masonry arch bridge assessment: Ring, Archie-M and the elasto-plastic-model, Wseas Transactions on Applied and Theoretical Mechanics, Issue 4, Vol. 5,2010, pp. 221-230.
7 A.H. Hendry, S.R. Davies, R. Royles, Test on a Stone, Masonry Arch at Bridgemill-Girvan, Transport and Road Research Lab, Contractor Report 7, UK,1985.
8- Tao, H., (2003), "The behavior of open spandrel brickwork masonry arch bridges" Ph.D. Thesis submitted to university of Salford, April 2003.
9- Garrity, S., W. "The rehabilitation of short span masonry arch highway bridges using near surface reinforcement" Proceedings of 8th International Conference on Short and Medium Span Bridges, Niagara Falls, Canada 2010
10- Al-Mamoori, M., Alwash, N. A. "Structural behavior of highly strength reinforced concrete beams with segmental arched bottom" IJCIET Journal,Volume 9,Issue 13,pp732-742.

DOI: http://doi.org/10.24086/aces2020/paper.183